OXFORD

Cerebral Cortex, 2022, 1–13
https://doi.org/10.1093/cercor/bhac414
Original Article

Default mode network scaffolds immature frontoparietal network in cognitive development

Menglu Chen[1,†], Ying He[1,†], Lei Hao[2,3,†], Jiahua Xu[1], Ting Tian[1], Siya Peng[1], Gai Zhao[1], Jing Lu[1], Yuyao Zhao[1], Hui Zhao[1], Min Jiang[1], Jia-Hong Gao[4,5], Shuping Tan[6], Yong He[1], Chao Liu[1], Sha Tao[1,*], Lucina Q. Uddin[7], Qi Dong[1], Shaozheng Qin[1,8,*]

[1]State Key Laboratory of Cognitive Neuroscience and Learning and IDG/McGovern Institute for Brain Research, Beijing Normal University, Beijing 100875, China,
[2]College of Teacher Education, Southwest University, Chongqing 400715, China,
[3]Qiongtai Normal University Key Laboratory of Child Cognition & Behavior Development of Hainan Province, Haikou 571127, China,
[4]Center for MRI Research, Academy for Advanced Interdisciplinary Studies, Peking University, Beijing 100871, China,
[5]McGovern Institute for Brain Research, Peking University, Beijing 100871, China,
[6]Beijing HuiLongGuan Hospital, Peking University, Beijing 100036, China,
[7]Department of Psychiatry and Biobehavioral Sciences, University of California at Los Angeles, Los Angeles, CA 90095, USA,
[8]Chinese Institute for Brain Research, Beijing 100069, China

*Corresponding authors: Shaozheng Qin and Shao Tao, State Key Laboratory of Cognitive Neuroscience and Learning & IDG/McGovern Institute for Brain Research, Beijing Normal University, XinJieKouWai Street, Beijing 100875, China. Email: szqin@bnu.edu.cn, taosha@bnu.deu.cn

†MC, YH, and LH contributed equally to this work.

The default mode network (DMN) is a workspace for convergence of internal and external information. The frontal parietal network (FPN) is indispensable to executive functioning. Yet, how they interplay to support cognitive development remains elusive. Using longitudinal developmental fMRI with an *n*-back paradigm, we show a heterogeneity of maturational changes in multivoxel activity and network connectivity among DMN and FPN nodes in 528 children and 103 young adults. Compared with adults, children exhibited prominent longitudinal improvement but still inferior behavioral performance, which paired with less pronounced DMN deactivation and weaker FPN activation in children, but stronger DMN coupling with FPN regions. Children's DMN reached an adult-like level earlier than FPN at both multivoxel activity pattern and intranetwork connectivity levels. Intrinsic DMN-FPN internetwork coupling in children mediated the relationship between age and working memory-related functional coupling of these networks, with posterior cingulate cortex (PCC)-dorsolateral prefrontal cortex (DLPFC) coupling emerging as most prominent pathway. Coupling of PCC-DLPFC may further work together with task-invoked activity in PCC to account for longitudinal improvement in behavioral performance in children. Our findings suggest that the DMN provides a scaffolding effect in support of an immature FPN that is critical for the development of executive functions in children.

Key words: default mode network; frontoparietal network; executive function; development.

Introduction

The human brain undergoes protracted development from childhood to adulthood, with significant improvement in a wide spectrum of learning, problem solving, and executive functions (Posner et al. 1988; Casey et al. 2005; Cole et al. 2014). Advances in developmental cognitive neuroscience have demonstrated that brain maturation, with strengthening and/or weakening connections among large-scale brain networks, lies at the foundation of cognitive development (Marek et al. 2015; Shine et al. 2016). In particular, functional interactions among regions of the default mode network (DMN, also known as medial frontoparietal network) (Uddin et al. 2019) and lateral frontal parietal network (FPN) are believed to play an integrative role in support of cognitive flexibility and adaptability to meet ever-changing environmental needs (Fair et al. 2007; Dosenbach et al. 2008; Vatansever et al. 2017). However, how functional coordination of these networks contributes to cognitive development in children remains elusive. Task-invoked engagement and disengagement, as well as coupling and decoupling among DMN and FPN regions involved in executive functioning such as working memory, have been especially well characterized (Vatansever et al. 2015; Sormaz et al. 2018), making them an ideal model for studying the fundamental organizing principles of these networks underlying cognitive development.

The DMN's contributions to human cognition are multifaceted. Early views posit that regions of the DMN decrease activity during externally demanding tasks such as working memory, while increasing activity during passive or internally-oriented task states (Buckner et al. 2008; Raichle et al. 2001). Moreover, DMN regions are sensitive to intrinsic information like belief, emotions and long-term memory (Yeshurun et al. 2021). Activity modulation of the DMN accounts for changes with age of long-term memory (Lustig et al. 2003; Nelson et al. 2016). Beyond these classical views, recent models from a topographic perspective suggest that the DMN, encompassing distributed transmodal regions (i.e. posterior cingulate cortex: PCC and medial prefrontal cortex: MPFC), is located at the top of the cortical hierarchy (Margulies et al. 2016; Sormaz et al. 2018) and plays an integrative role in support of

Received: January 28, 2022. **Revised:** September 15, 2022. **Accepted:** September 16, 2022

human cognition and behavior. Its relative isolation from sensorymotor and perceptual systems permits neurocognitive operations less tethered to environmental inputs (Buckner and Krienen 2013; Smallwood et al. 2021), thereby allowing more abstract representations to emerge (Haggard 2008; Margulies et al. 2016). Greater coupling between PCC with regions in executive function systems has been observed, while its activation is reduced during a semantic cognition task (Krieger-Redwood et al. 2016), suggesting the contribution of PCC (a core node of the DMN) to executive function. Nuanced functional interactions between the DMN and FPN have been implicated in a wide range of executive functions involving information maintenance and updating processes that are critical for working memory (Fornito et al. 2012; van Buuren et al. 2019). The majority of previous fMRI studies have focused on how the FPN contributes to working memory processing (Fair et al. 2007; Supekar et al. 2009; Satterthwaite et al. 2013). Enhanced activation and functional connectivity in FPN regions are associated with developmental improvement in executive functioning (Johnson 2011; Satterthwaite et al. 2013; Sherman et al. 2014). Yet, it remains unclear how functional coupling and decoupling between DMN and FPN contribute to working memory development in children. Given its unique neuroanatomical features and topographic organization, one may conjecture that DMN regions would play a role in cognitive development.

From a developmental perspective, recent studies have demonstrated that the DMN tends to be a cohesive connector system with increasing internal coherence and high integration with the FPN, salience, and memory networks between the ages of 8 and 22 (Gu et al. 2015). Core regions of the DMN are connected at ages 7–9 and keep integrating into a cohesive network (Fair et al. 2008) with the fastest development in long-range connectivity between the PCC and medial prefrontal cortex (Fair et al. 2008; Power et al. 2010). Moreover, the DMN exhibits both high within- and between-network coupling, while the FPN shows relatively lower within-network coupling over 8–22 years old (Gu et al. 2015), suggesting distinct developmental trajectories of these functional brain networks. Thus, findings from structural and functional MRI studies have demonstrated that the FPN regions undergo protracted development (Johnson 2001; Klingberg et al. 2002; Olesen et al. 2003; Alvarez and Emory 2006; Fair et al. 2007), with slower maturation than the DMN from childhood to adulthood (Supekar et al. 2010). Although developmental changes in the neuroanatomical properties of the DMN regions have been investigated in children and adults (Uddin et al. 2011), little is known about their contributions to working memory development.

Human functional brain networks are recognized to possess high flexibility and adaptability, as they can be flexibly reconfigured to compensate for certain cognitive functions when some systems are immature, affected by age-associated decline, and/or impaired (Mürner-Lavanchy et al. 2014; Hartwigsen 2018; Spreng and Turner 2019). Across the life span, the human brain is an adaptive system that engages in compensatory scaffolding in response to the challenges posed by declining neural structures and function affected by age-associated factors, and/or impairment (Park and Reuter-Lorenz 2009). Scaffolding is a normal process present across the lifespan that involves use and development of complementary, alternative neural circuits to achieve a particular cognitive goal ("compensatory scaffolding") (Park and Reuter-Lorenz 2009). Such a compensatory scaffolding mechanism has been reported by many neuropsychological and neuroimaging studies in children and adults (Di Martino et al. 2014; Mürner-Lavanchy et al. 2014; Ivanova et al. 2017). One fundamental question in human developmental cognitive neuroscience is to understand how brain systems and networks that mature earlier could provide a scaffold for those that mature relatively later to support cognitive development. At a behavioral level, children's more frequent use of embodied procedures that mature early such as self-involved rehearsal and episodic memory can indeed scaffold the protracted development of advanced problem-solving skills (Siegler 1996; Butterworth 1999; Qin et al., 2014). Recent studies in adults demonstrate that virtual lesions of language regions result in less deactivation of DMN regions, which likely reflects recruitment of general mental resources when task demands increase (Hartwigsen 2018). Aging studies have also revealed that an increased recruitment of the DMN during external tasks could help prevent age-related cognitive decline (Spreng and Schacter 2012). Moreover, older adults exhibit higher functional coupling between regions in the DMN and FPN (Kupis et al. 2021) compared with young adults during cognitive control and creativity tasks (Spreng and Turner 2019). These findings suggest that the DMN may compensate for the earlier decline of FPN regions critical for higher order cognitive functions (e.g. working memory) in aging. From a developmental perspective, it is thus reasonable to speculate that the DMN would provide a scaffold for an immature FPN in executive functioning. However, how the DMN could exert a scaffolding role in support of the FPN during working memory in the developing brain remains unexplored.

To address the above questions, we implemented developmental functional magnetic resonance imaging (fMRI) with an *n*-back working memory paradigm and a longitudinal design spanning age 6–15 years in 528 typically developing children and 103 adults (age 18–28 years). A numerical *n*-back working memory task (Fig. 1A) with 0-, 1-, and 2-back conditions was used to characterize longitudinal improvement in working memory performance, and its associated activation and deactivation in the FPN and DMN from childhood to adulthood. A set of multivoxel activity analyses were conducted to assess adult-like maturation metrics for the DMN and FPN. This approach takes advantage of examining similarities between multivoxel activity patterns in children and activity patterns in mature adults, rather than absolute levels of activity, thus removing concerns about activation/deactivation levels within DMN and FPN regions (Kriegeskorte et al. 2008, Zhuang et al. 2022). A network connectivity approach was then used to examine maturational changes in intra- and inter-network functional organization among DMN and FPN regions both during task-dependent and task-free states. In line with brain maturation and recent neurocognitive models of the DMN, we hypothesized that we would observe heterogeneous developmental profiles of working memory-related activity patterns and network properties within DMN and FPN regions from childhood to adulthood and that the DMN would scaffold the slower maturity of the FPN to support working memory development during childhood.

Methods and materials

Participants

A total of 631 participants were included in this study: 528 typically developing children aged 6–15 years (mean ± standard deviation [SD] = 9.26 ± 1.45) at visit 1, 300 children about 1.09 year later at visit 2, 172 children about 2.06 years later at visit 3, and 103 young healthy adults aged 18–28 years (mean ± SD = 22.7 ± 2.34) (Tables S1 and S2). Neuroimaging and behavioral data were obtained from the Children School Functions and Brain Development Project (CBD, Beijing Cohort). Written informed consent was obtained before the experiment from each participant. For

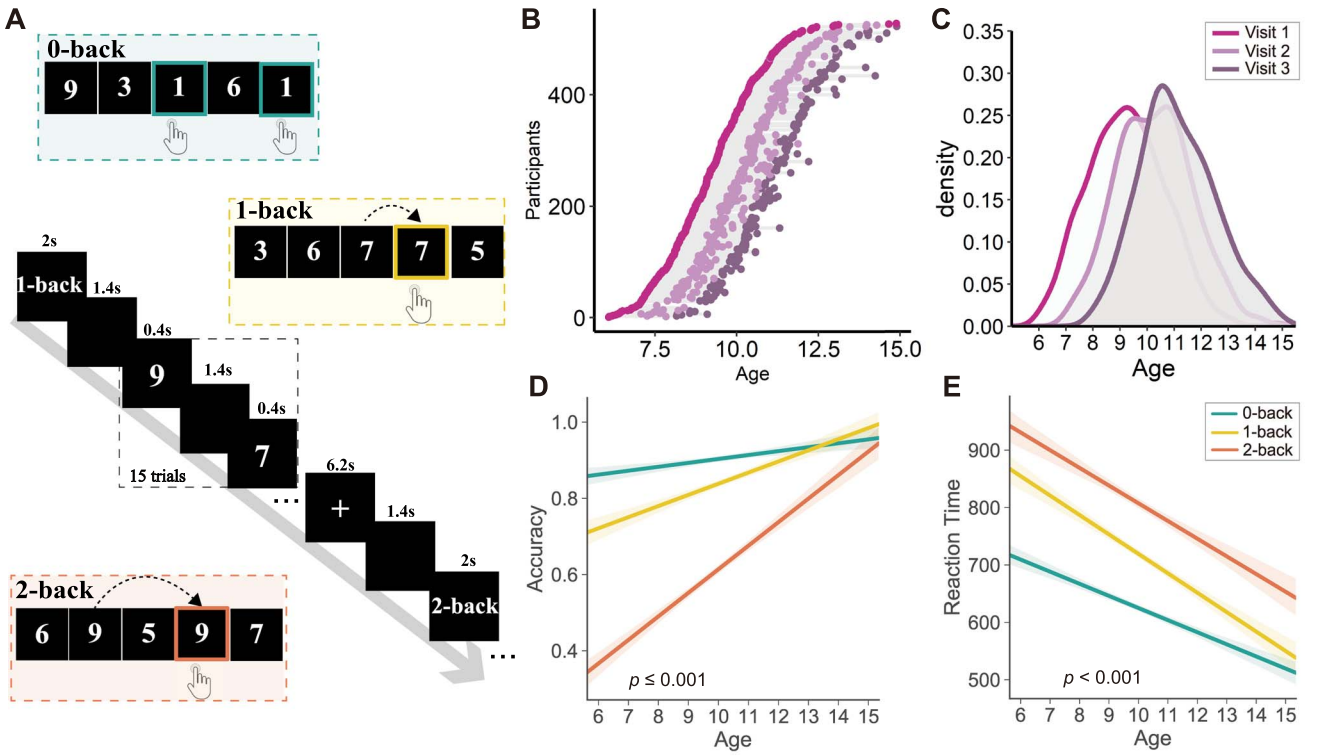

Fig. 1. Experimental paradigm and longitudinal improvement in working memory performance from age 6 to 15. A) Numerical 0-, 1-, and 2-back working memory task conditions. B and C) Age distribution of children at 3 visits, each dot represents one child at each visit. D and E) Line curves depict significant longitudinal improvement in working memory accuracy (all $t \geq 3.36$, $P \leq 0.001$) and RTs (all $t \leq -7.19$, $P < 0.001$) as a function of age at 3 working memory loads from 6 to 15 years of age.

children, written informed consent was obtained from one of the parents or legal guardians. The procedures of consent and experiment were approved by local ethics in accordance with the standards of the Declaration of Helsinki. All of the participants reported no history of vision problems, no history of neurological, or psychiatric disorders, and no current use of any medication or recreational drugs. Demographics of children and adults are listed in Tables S1 and S2. Only 604 participants underwent fMRI scanning at visit 1 (501 children and 103 adults); those with either incomplete task/field map scanning (42 children and 9 adults) or excessive head motion with max displacement larger than one voxel size (3.5 mm) (35 children and 1 adult) were excluded from further neuroimaging data analyses. There were 229 children scanning at visit 2 and 122 children at visit 3.

Cognitive task

A block-design of a numerical *n*-back task was used to assess children's working memory capacity during scanning (Fig. 1A). Participants completed 12 blocks of random alternating three loads (i.e. 0-, 1-, and 2-back) interleaved by a jittered fixation for random variable duration of between 8 and 12 s. Within each block, a sequence consisting of 15 single digits was presented centrally on the screen. Each digit was presented for 400 ms followed by an interstimulus interval of 1,400 ms. Each block lasted 27 s and started with a 2-s instruction for indicating the block was 0-, 1-, or 2-back condition. During the 0-back condition, participants were asked to detect whether the current item on the screen was "1" or not. During the 1-back condition, participants were asked to respond whether the current item was the same as the previous one. During the 2-back condition, participants were asked to detect whether the current item had appeared 2 positions back in the sequence. Participants were instructed to make a button press as quickly and accurately as possible with their index finger when detecting a target. Before fMRI scanning, they were extensively trained in performing the task to minimize interindividual variability and reduce practice effects. Stimuli were presented via E-Prime 2.0 (http://www.pstnet.com; Psychology Software Tools, Inc).

Behavioral data analysis

Participant demographic data and behavioral measures were analyzed with the R package (version 3.5.0). Accuracy was calculated by subtracting false alarm rate from hit rate. Both accuracy and RTs were obtained for each participant. Cross-sectional comparisons between children and adults were performed to examine developmental differences in working memory performance during 0-, 1-, and 2-back conditions (Fig. S1). Pearson correlation analysis was used to investigate age-related changes in accuracy and RTs in three conditions in 6- to 15-year-old children (Figs. S2 and S3). Longitudinal improvement was characterized by the Z-score of difference in RTs in the 2-back condition at visit 1 minus visit 3. Combining cross-sectional and longitudinal analyses allowed us to investigate the linear relationship between age and development of working memory performance in childhood.

To investigate longitudinal improvements in behavioral performance, we used a linear mixed model to characterize age-related effects on working memory performance. The nlme package in R (Pinheiro et al. 2018; Team 2018) was used to investigate the effect of age on longitudinal changes in working memory performance. We characterized the fitting model using the following equation:

$$\text{Linear age model}: Y = \text{intercept} + \text{random}\ (\text{participants ID}) + \text{age} + \text{error}.$$

Imaging data acquisition

Whole-brain images were acquired from a Siemens 3.0 T scanner (Magnetom Prisma syngo MR D13D, Erlangen, Germany) using a 64 head coil with a T_2*-sensitive echo-planar imaging sequence based on blood oxygenation level-dependent contrast. Thirty-three axial slices (3.5-mm thickness, 0.7-mm skip) parallel to the anterior and posterior commissure line and covering the whole brain were imaged with the following parameters: repetition time (TR) 2000 ms, echo time (TE) 30 ms, flip angle (FA) 90°, voxel size $3.5 \times 3.5 \times 3.5$ mm^3, and field of view (FOV) 224×224 mm^2. A resting state scan consisting of 240 volumes was acquired, and followed by the *n*-back task consisting of 232 volumes. In addition, each participant's high-resolution anatomical images were acquired through 3D sagittal T_1-weighted magnetization-prepared rapid gradient echo with a total of 192 slices (TR 2530 ms, TE 2.98 ms, FA 7°, inversion time 1100 ms, voxel size $1.0 \times 1.0 \times 1.0$ mm^3, acquisition matrix 256×224, FOV 256×224 mm^2, BW 240 Hz/Px, slice thickness 1 mm).

fMRI data preprocessing

Brain images were preprocessed using statistical parametric mapping (SPM12, https://www.fil.ion.ucl.ac.uk/spm/software/spm12/) (Friston et al. 1994) based on MATLAB software platform (version 8.1; MathWorks Inc., Natick, MA, USA). The first 5 volumes of resting state scans and the first 4 volumes of *n*-back task scans were, respectively, discarded for signal equilibrium and participants' adaptation to scanner noise. The remaining images were corrected for slice acquisition timing and realigned for head motion correction. Subsequently, they were co-registered to each participant's gray matter image segmented from the corresponding high-resolution T_1-weighted image, then spatially normalized into a common stereotactic Montreal Neurallogical Institute space and resampled into 2-mm isotropic voxels. Finally, images were smoothed using an isotropic 3D gaussian kernel with 6-mm full-width half-maximum.

Univariate general linear model analysis

To assess task-invoked neural activity in distinct working memory load processes, the three conditions (i.e. 0-, 1-, and 2-back) were modeled as 3 regressors separately and convolved with the canonical hemodynamic response function (HRF) implemented in SPM12. In addition, each participant's motion parameters (3 translational motions and 3 rotary movements) from the realignment procedure were included to regress out potential effects of head movement (HM) on brain response. We included high-pass filtering using a cutoff of 1/128 Hz, and corrections for serial correlations in fMRI using a first-order autoregressive model (AR(1)) in the GLM framework.

Relevant contrast parameter estimate images were initially generated at the individual-subject level, and then submitted to 2 (Group: children vs. adults)-by-3 (Loads: 0-, 1-, vs. 2-back) ANOVA in the group analysis. Significant clusters of main effect of Loads were determined by using a stringent threshold of $P < 0.001$ with family-wise error (FWE) corrections for multiple comparisons. We also conducted 1-way ANOVAs with 6 different age groups to examine age-specific brain activation patterns as a function of age from 6 to 12 years during childhood as well as in adults. For visualization purposes, significant clusters were determined using a stringent threshold of $P < 0.001$ and an extent threshold of $P < 0.05$ corrected for multiple comparisons based on suprathreshold cluster-size distributions computed by Monte Carlo simulations.

Regions of interest definition

To define regions of interest (ROIs) for the DMN and FPN, we undertook several steps by combining the masks derived from the NeuroSynth platform (http://NeuralSynth.org) and working memory-related activation maps across all participants (including children and adults) in the present study. First, we used the NeuroSynth platform for large-scale, automated synthesis of fMRI data with "working memory" and "default mode network" as search terms and then download an association mask at the whole brain level. Second, we decomposed the working memory-related activation map involved in the 2-back condition across children and adults into a positive activation map and a negative activation map using a stringent threshold of $P < 0.001$ with FWE corrections for multiple comparisons. Third, the DMN and FPN ROIs were generated by overlapping maps of term-related and working memory-related activation. These ROIs in the DMN consisted of the ventral medial prefrontal cortex (vmPFC), PCC, bilateral angular gyrus (AG_L, AG_R), and bilateral parahippocampal gyrus (PHG_L, PHG_R). ROIs in the FPN included the bilateral dorsal lateral prefrontal cortex (DLPFC_L, DLPFC_R), bilateral inferior frontal gyrus (IFG_L, IFG_R), and bilateral inferior parietal lobule (IPL_L, IPL_R) (Table. S3). Parameter estimates (or beta weights) were then extracted from these ROIs in all participants for subsequent analyses (Figs.S4 and S5).

Multivariate maturation index

To investigate longitudinal maturational changes in neural activity patterns of working memory-related DMN and FPN during childhood, an overall multivariate maturation index for each of 3 conditions using representation similarity analysis (RSA; Kriegeskorte et al. 2008) was computed to assess the degree of each working memory-related multivoxel neural activity pattern similarity in each child relative to the mature template of corresponding neural activity patterns averaged across adults. Each working memory condition multivoxel pattern vector was extracted from each child from 3 visits and averaged adults, respectively, by the mask of DMN and FPN (defined above). We then computed the multivariate maturation index using Pearson's correlation between condition-specific patterns vector in each child and the corresponding reference vector in the adult brain (Fig. 2A). A linear mixed-effect model of the maturation index was used to estimate longitudinal developmental changes as a function of age from 6 to 15 years for the DMN and FPN in 0-, 1-, and 2-back separately (Figs. S6 and S7), in which the gender and HM of each subject were included as covariates in the model.

$$\text{Linear age model}: Y = \text{intercept} + \text{random}\ (\text{participants ID}) + \text{age} + \text{gender} + \text{HM} + \text{error}.$$

Working memory-related functional coupling analysis

Functional coupling maps were generated by applying the generalized psychophysiological interactions (gPPI) analysis in each working memory condition (McLaren et al. 2012). Pairwise task-dependent functional coupling for 12 ROIs was computed to create a 12-by-12 matrix in each working memory condition for all children and adults (Fig. S8). The gPPI analysis is widely used to assess task-dependent functional connectivity of a specific seed ROI with the rest of the brain after removing potential confounds of overall task activation and common driving inputs. Specifically, mean time series from each seed ROI were extracted and then

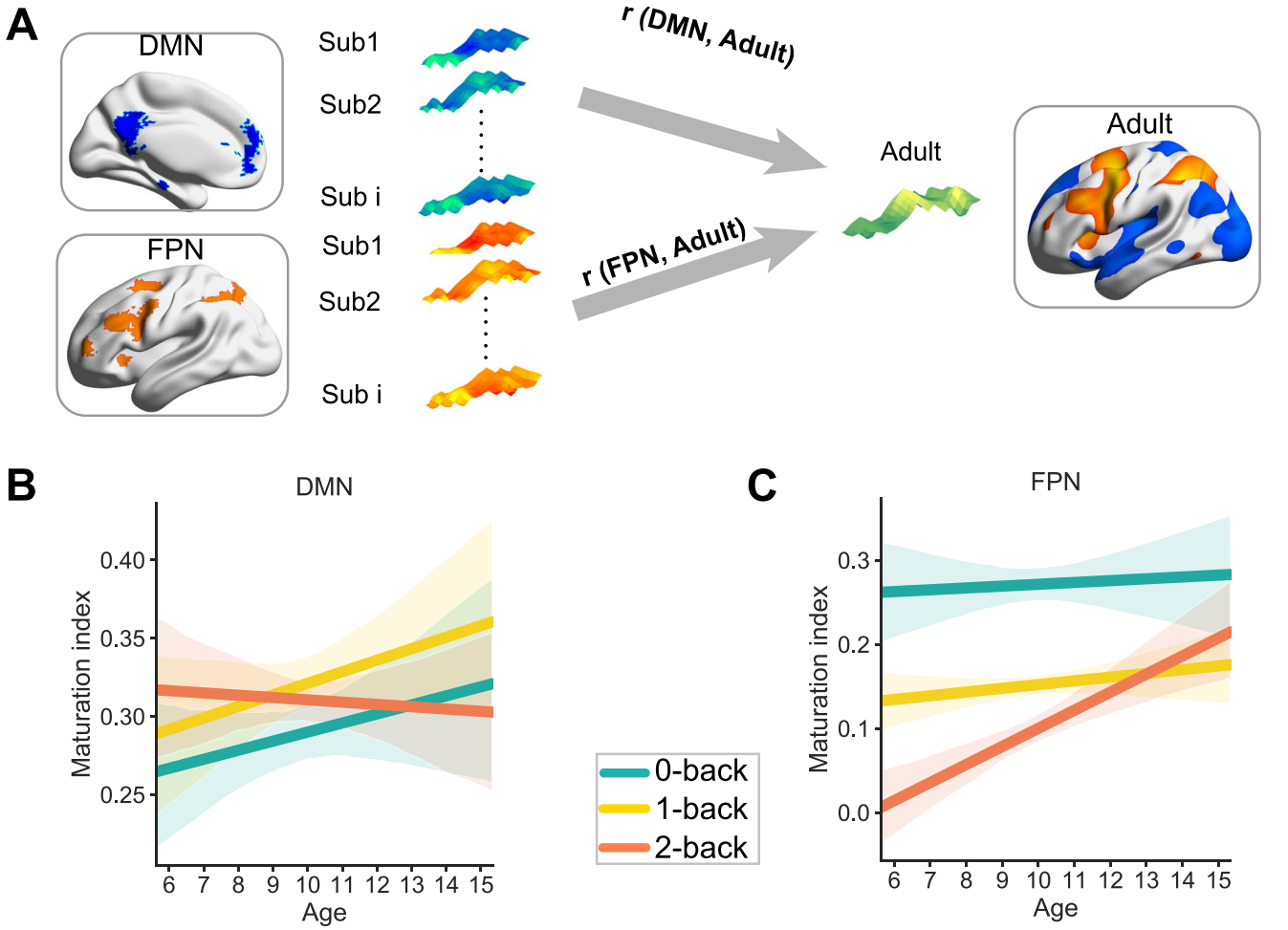

Fig. 2. Age-related longitudinal changes in working memory-related multivoxel activity patterns in DMN and FPN. A) A schematic illustration of multivariate maturation indices, derived by computing multivoxel pattern similarity of working memory-related activity patterns within the DMN (or FPN) mask relative to the mature template derived from average activity patterns in the DMN and FPN relative to the averaged mature activity across adults. B and C) Line curves fit the age-related longitudinal changes in maturation indices in DMN (all $t > -1.55$, $P > 0.12$) and FPN (0- and 1-back: $T > -1.46$, $P > 0.15$, 2-back: $T = 2.43$, $P = 0.015$) for all children at 3 visits in each working memory condition.

deconvolved in order to uncover neuronal activity (i.e. physiological variable) and multiplied with the task design vector contrasting the experimental conditions versus the fixation condition (i.e. a binary psychological variable) to form a psychophysiological interaction (PPI) vector. To form the PPI regressor of interest, this interaction vector was convolved with a canonical HRF in SPM12. The psychological variable representing task design as well as mean-corrected time series of each seed ROI were also included in the GLM to remove overall task-dependent activation and the effects of common driving inputs including head motion parameters on brain connectivity. Note that only the voxels within the 12 ROIs were included in this analysis.

Intrinsic functional connectivity analysis

Pairwise task-free intrinsic functional coupling for 12 ROIs was computed to construct a 12-by-12 matrix for all children and adults based on resting fMRI data (Fig. S8). Regional time series of 12 ROIs were extracted from data filtered with a bandpass temporal filter (0.008–0.10 Hz). Each time series was then submitted into the individual-level analysis. White matter signal, cerebrospinal fluid signal, and six head-motion parameters were included as nuisance covariates in the general linear model. Pearson correlation maps were produced by computing pairwise correlations of the 12 ROIs. Each ROI region was a 6-mm diameter sphere centered on our activation results foci (Table S3).

Intra- and inter-network functional coupling analysis

We partitioned children and adults' group-averaged matrices into 2 subnetworks of the DMN and FPN by averaging each connection within the nodes in FPN or in DMN. By averaging the connections between nodes in DMN and FPN, we calculated the internetwork coupling of each participant. We then investigated developmental changes in connectivity strength within and between these subnetworks for both task-dependent and task-free data. These within- and between-network metrics in each of 3 working memory load conditions were submitted to 2-by-3 repeated-measure ANOVAs with Group (children vs. adults) as a between-subject factor and Condition (0-, 1-, vs. 2-back) as a within-subject factor. A correlation analysis in task-free connectivity was also conducted to measure age-related changes in intrinsic connectivity strength.

To further characterize the developmental differences and which edges drive the difference of intrinsic and working memory-related functional network coupling between children and adults, we compared functional coupling by conducting separate independent *t*-tests to examine differences between

groups for each edge in both resting and 2-back conditions. After false discovery rate (FDR) correction ($P < 0.05$) for multiple comparisons, we found 26 edges in intrinsic connectivity and 9 edges in working memory-related functional connectivity that had significant differences between children and adults (Fig. S9).

Mediation analysis

The mediation models and statistical tests were conducted in SPSS version 21 using PROCESS (IBM Corp., Armonk, NY) (Hayes 2013), which is based on regression analysis. The significance of the indirect or mediated effect was assessed using 5,000 bias corrected bootstrapping (Preacher and Hayes 2008). The indirect effect was considered significant if the 95% confidence interval (CI) did not include zero.

Results

Developmental improvement of working memory performance in children

First, we investigated developmental differences in working memory performance between children (year 1) and adults. Separate ANOVAs for accuracy and reaction times (RTs) were conducted with working memory Loads (0-, 1-, vs. 2-back) as a within-subject factor and Group (children vs. adults) as a between-subject factor. These analyses revealed Loads-by-Group interaction effects ($F_{(2,860)} \geq 14.7$, $P < 0.001$) and main effects of loads ($F_{(2,860)} \geq 232.6$, $P < 0.001$) and Group ($F_{(1,430)} \geq 167$, $P < 0.001$) for both accuracy and RTs. Follow-up t-tests revealed that children had lower accuracy ($t_{(430)} \geq 5.39$, $P < 0.001$, Cohen's $d \geq 0.61$) and longer RTs ($t_{(432)} \leq -10.6$, $P < 0.001$, Cohen's $d \leq -1.20$) in the 3 conditions as compared with adults (Fig. S1).

We then investigated longitudinal improvement in working memory performance over development from age 6–15 years for accuracy and RTs of each condition in children. Using a linear mixed-effect model, we observed a significant linear increase in accuracy for 3 working memory loads over development ($t \geq 3.36$, $P \leq 0.001$). For RTs, we observed a prominent linear decrease in 3 working memory loads ($t \leq -7.19$, $P < 0.001$) over development (Fig. 1D and E). These results indicate inferior working memory performance in children than adults, with a longitudinal improvement from 6 to 15 years of age.

Adult-like working memory-related multivoxel activity pattern in DMN but not in FPN in children

Next, we investigated age-related changes in brain systems involved in working memory processing in children between 6 and 15 years of age. As shown in Fig. 2A, we observed prominent age-related increases in task-evoked brain activity in the DMN and FPN regions, especially for the 2-back condition in children. Further analyses of brain activity patterns among 3 working memory load conditions in children and adults revealed less pronounced functional dissociation of activation patterns in DMN and FPN among 3 working memory loads in children than adults (Fig. S5A and B). Moreover, the most prominent effect was observed in the 2-back condition, with stronger activation in FPN regions and more deactivation in DMN regions both in children and adults (Fig. S5C).

We further computed an overall multivariate maturation index to quantify the longitudinal developmental profile of these 2 brain systems including all children's imaging data at 3 visits. A first step was to create the masks for the DMN and FPN from NeuroSynth platform (see Methods) (Fig. 2A). The maturation index for each working memory load condition was then represented by the similarity of each child's condition-specific pattern vector in DMN and FPN relative to the mature pattern represented by an averaged pattern vector in the corresponding mask in adults. Linear mixed-effect models revealed no significant age-related change as regards the maturation index in the DMN for all of three working memory load conditions (all $t > -1.55$, $P > 0.12$). The maturation index in the FPN showed a flat pattern in 0-back and 1-back ($t > -1.46$, $P > 0.15$) but a linear increase as a function of age from 6 to 15 years in 2-back ($t = 2.43$, $P = 0.015$) conditions (Fig. 2B and C; Figs. S6 and S7). These results indicate that working memory-related multivoxel pattern similarity in the DMN reaches an adult-like level early in development, whereas activity patterns in the FPN undergo protracted development during childhood.

Adult-like working memory-related intranetwork coupling in DMN but not in FPN in children

To track developmental differences in working memory-related intra- and internetwork functional coupling in DMN and FPN between children and adults, we constructed a network consisting of 12 × 12 pairwise links for DMN and FPN regions for each condition, using a generalized form of context-dependent psychophysiological interactions (gPPI). Intranetwork coupling metrics were computed for nodes within the DMN and FPN, respectively (Fig. 3A–C). We then conducted separate 2 (Group: children vs. adults)-by-3 (Loads: 0-, 1-, vs. 2-back) ANOVAs for DMN and FPN intranetwork coupling metrics.

For intranetwork coupling of the DMN, we observed a significant interaction effect ($F_{(2,688)} = 3.34$, $P = 0.036$) and a main effect of working memory loads ($F_{(2,688)} = 23.46$, $P < 0.001$), but no significant effect of Group ($F_{(1,344)} = 3.40$, $P = 0.066$) (Fig. 3D). Follow-up t-tests revealed a prominent load effect only in the 2-back condition (2- vs. 0-back: $t_{(688)} = -6.22$, $P < 0.001$; 2- vs. 1-back: $t_{(688)} = -5.60$, $P < 0.001$, both Cohen's $d < -0.43$) but not between 1- and 0-back conditions ($t_{(688)} = 0.62$, $P = 0.54$, Cohen's $d = 0.047$). In other words, intranetwork coupling in DMN nodes decreases as load increases in children and adults. But intranetwork coupling of DMN in 2-back condition displays no difference between children and adults ($t_{(792)} = 0.20$, $P = 0.84$, Cohen's $d = 0.01$).

Parallel analyses for intranetwork coupling of FPN revealed a marginally significant interaction between Group and Loads ($F_{(2,688)} = 2.60$, $P = 0.075$), and significant main effects of Group ($F_{(1,344)} = 5.10$, $P = 0.025$) and Loads ($F_{(2,688)} = 4.23$, $P = 0.015$) (Fig. 3E). Follow-up 1-way ANOVA revealed no difference among 3 loads in children ($F_{(2,504)} = 0.21$, $P = 0.810$), but significant working memory-load effect in adults ($F_{(2,184)} = 5.87$, $P = 0.003$), with stronger coupling within FPN regions as load increases (1- vs. 0-back: $t_{(184)} = 2.92$, $P = 0.004$, Cohen's $d = 0.43$; 2- vs. 0-back: $t_{(184)} = 3.01$, $P = 0.003$, Cohen's $d = 0.44$, 2- vs. 1-back: $t_{(184)} = 0.09$, $P = 0.93$, Cohen's $d = 0.01$). These results indicate that children exhibit an adult-like intranetwork coupling in DMN regions but weaker intranetwork coupling in the FPN when compared with adults.

Age-related increase in DMN-FPN internetwork coupling during working memory was mediated by intrinsic functional connectivity

Given that long-range connections of large-scale brain networks undergo protracted development from childhood to adulthood (Supekar et al. 2009; Grayson and Fair 2017), we further investigated developmental changes in working memory-related functional coupling between DMN and FPN in children and adults. A 2 (Group: children vs. adults)-by-3 (Loads: 0-, 1-, vs. 2-back) ANOVA for internetwork coupling of DMN and FPN revealed a significant

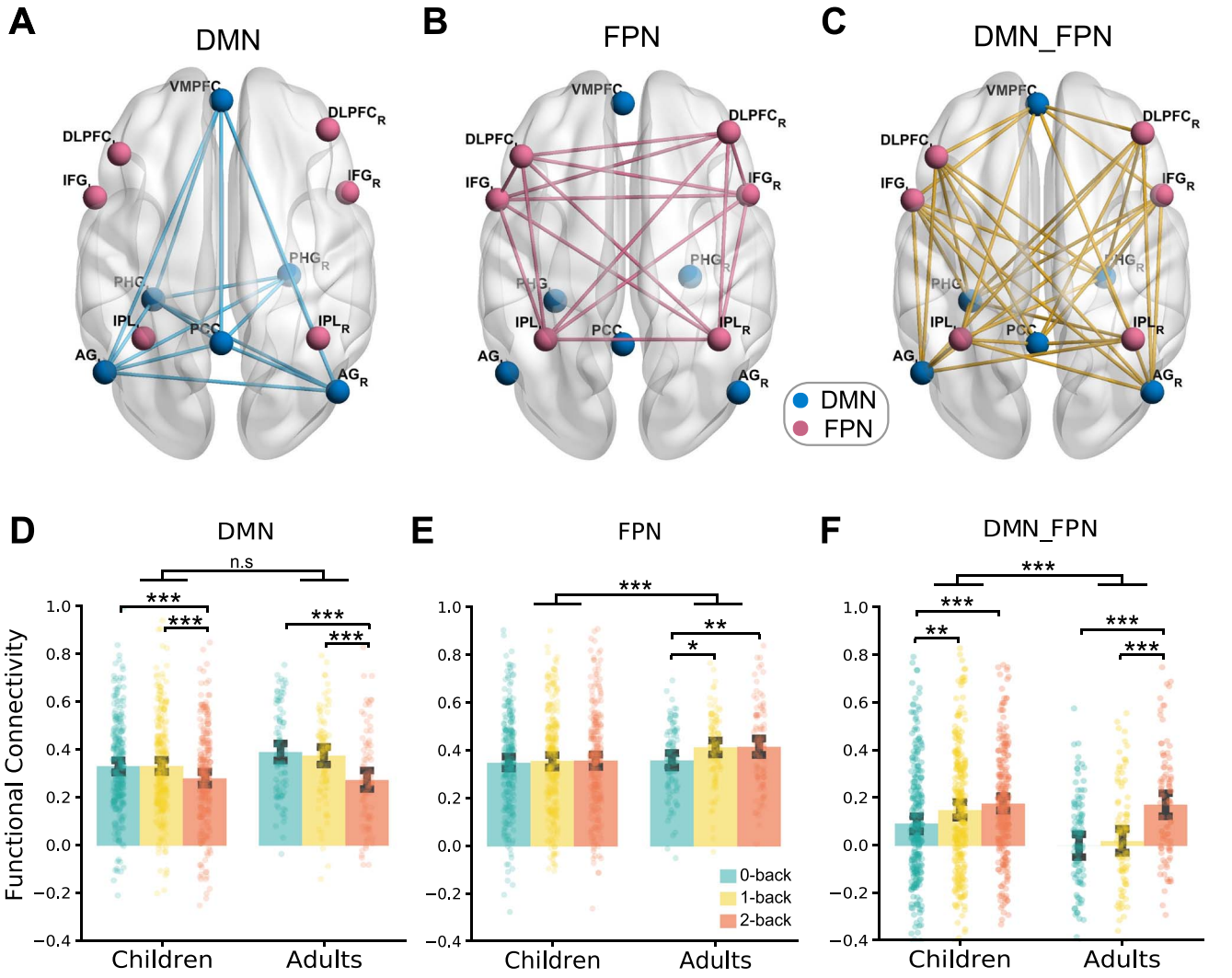

Fig. 3. Developmental differences in intra- and internetwork coupling of the DMN and FPN during working memory between children and adults. A–C) An illustration of intranetwork coupling within DMN and FPN, as well as internetwork DMN-FPN coupling. D) Bar graphs depict a main effect of working memory loads for DMN-intranetwork coupling in both children and adults, with an adult-like level in children relative to adults. E) Bar graphs depict a main effect of working memory loads for FPN intranetwork coupling in adults but not children, with weaker coupling in children than adults. F) Bar graphs depict a main effect of working memory loads for DMN-FPN internetwork coupling in both children and adults, with stronger DMN-FPN coupling in children than adults. Notes: N.s., not significant; *, $P < 0.05$; **, $P < 0.01$; ***, $P < 0.001$.

Group-by-Loads interaction ($F_{(2, 688)} = 7.63$, $P < 0.001$) as well as significant main effects of Loads ($F_{(2, 688)} = 30.57$, $P < 0.001$) and Group ($F_{(1, 344)} = 9.85$, $P = 0.002$). Post-hoc *t*-tests revealed higher DMN-FPN coupling as working memory load conditions increase in children (statistics listed in Table S4) (Fig. 3F). When compared to adults, children exhibited stronger internetwork coupling between DMN and FPN for low and moderate, but not high, task demands.

We then further investigated developmental differences in intrinsic intra- and internetwork of DMN and FPN between children and adults, by analysis of resting-state fMRI data for network matrices among 12 ROIs. Parallel 2-by-3 ANOVA revealed a significant Group-by-Network interaction effect ($F_{(2, 648)} = 18.7$, $P < 0.001$), a main effect of Network ($F_{(2, 648)} = 1073.6$, $P < 0.001$), but no main effect of Group ($F_{(1, 324)} = 0.22$, $P = 0.64$) (Fig. 4A–C). Post hoc *t*-tests revealed no difference in DMN intrinsic coupling between children and adults ($t_{(785)} = -0.86$, $P = 0.39$, Cohen's $d = -0.06$). However, children exhibited lower FPN intrinsic functional coupling ($t_{(785)} = -2.38$, $P = 0.018$, Cohen's $d = -0.17$) than adults. Children also exhibited higher internetwork coupling than adults ($t_{(785)} = 4.30$, $P < 0.001$, Cohen's $d = 0.31$). These results again indicate heterogeneous integration in DMN and FPN from 6 to 12 years of age during childhood, with adult-like integration of DMN, weaker coupling in FPN, but higher coupling between DMN and FPN when compared with adults.

Given children's higher DMN-FPN coupling both during working memory and resting states, we further implemented a mediation analysis to test whether intrinsic DMN-PFN coupling at rest would affect age-related changes in internetwork coupling during working memory tasks. This analysis revealed an indirect mediatory effect of children's DMN-FPN intrinsic coupling (indirect estimate = −0.008, $P < 0.05$, 95% CI = [−0.016, −0.003] on age-related DMN-FPN coupling during working memory (Fig. 4D). Pearson's correlation analysis further confirmed a significant positive correlation between working memory-related DMN-FPN functional coupling and accuracy in the 2-back condition in children ($r = 0.14$, $P = 0.03$), but not adults ($r = 0.09$, $P = 0.41$) (Fig. 4E). Altogether, these results indicate that children's stronger intrinsic DMN-FPN coupling mediates an indirect relationship between age and DMN-FPN internetwork coupling during working memory processing.

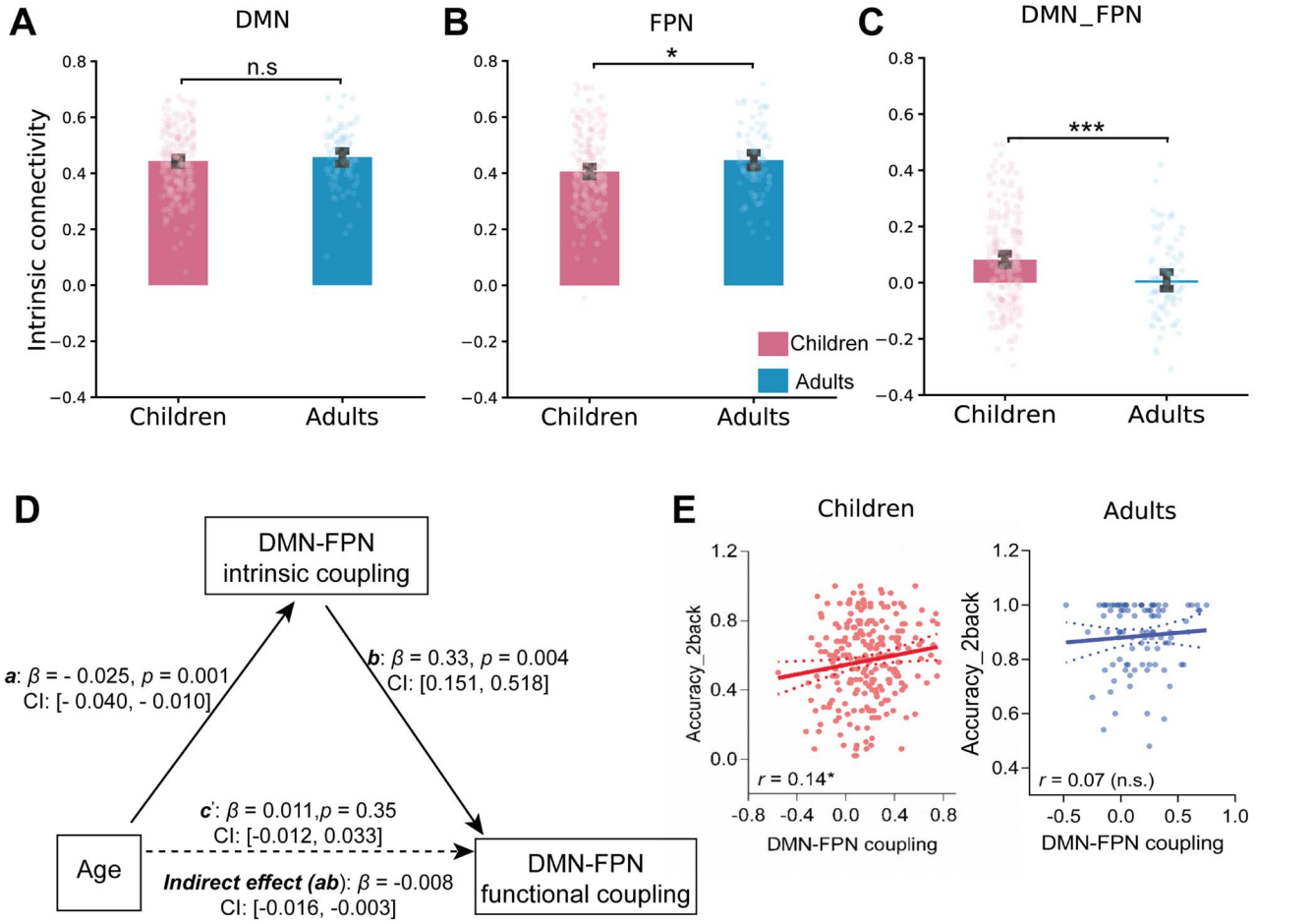

Fig. 4. Developmental differences in intrinsic intra- and internetwork coupling of the DMN and FPN between children and adults. A) Bar graphs depict no difference in intrinsic intra-network coupling in DMN between children and adults. B) Bar graphs depict weaker intrinsic intranetwork coupling in FPN in children than adults. C) Bar graphs depict stronger DMN-FPN intrinsic coupling in children than adults. D) A mediation model shows the mediating effect of children's intrinsic DMN-FPN coupling that could account for an indirect association between age and DMN-FPN coupling during working memory. E) Scatter plot depicts higher working memory-related DMN-FPN functional coupling predictive of better accuracy in the 2-back task in children but do not have significant correlation in adults. Notes: N.s., not significant; *, $P < 0.05$; ***, $P < 0.001$.

Intrinsic PCC-DLPFC coupling and task-invoked activity in PCC predicts children's longitudinal working memory improvement

To further characterize which functional pathways drive children's age-related increases in internetwork coupling involved in working memory processing, we conducted separate independent *t*-tests to examine group differences in connectivity strength for each link during both resting state and 2-back conditions (Fig. 5A and B). After FDR correction, we observed that children showed higher task-free intrinsic ($t_{(324)} = 2.86$, $P_{(corrected)} = 0.017$, Cohen's $d = 0.36$) as well as task-invoked functional coupling between PCC and the left DLPFC in the 2-back condition ($t_{(344)} = 3.12$, $P_{(corrected)} = 0.026$, Cohen's $d = 0.38$) than adults. We then implemented a mediation analysis to test whether children's intrinsic functional coupling accounts for age-related increase in PCC-DLPFC functional coupling during working memory. This analysis revealed an indirect mediatory effect of intrinsic PCC-DLPFC coupling (indirect estimate = −0.007, $P < 0.05$, 95% CI = [−0.019, −0.001]) on strengthening functional coupling involved in the 2-back working memory task (Fig. 5C).

To test how DMN-FPN pathways and their task-evoked activity account for children's longitudinal improvement in working memory performance, we further implemented a mediation analysis to investigate whether intrinsic PCC-DLPFC coupling along with task-evoked PCC activity could mediate the relationship between age and longitudinal improvement in performance. Longitudinal improvement was measured by children's RTs in the 2-back condition at visit 1 minus visit 3, as the greater RTs difference represents greater longitudinal improvement. As shown in Fig. 5D, this analysis revealed a chain mediating pathway (indirect estimate = −0.006, $P < 0.05$, 95% CI = [−0.023, −0.001]). That is, as children's age increased, intrinsic PCC-DLPFC coupling and task-evoked activity decreases in PCC during the 2-back condition could indirectly account for longitudinal improvement in working memory performance about 2 years later. Altogether, these results indicate that intrinsic PCC-DLPFC coupling and activity in PCC were associated with improvements in working memory performance during development.

Discussion

The mechanisms of DMN and FPN interplay supporting working memory development are incompletely understood. By leveraging task-dependent and task-free fMRI with a longitudinal design, we investigated this question in a large sample of children and adults. Behaviorally, children's working memory performance underwent

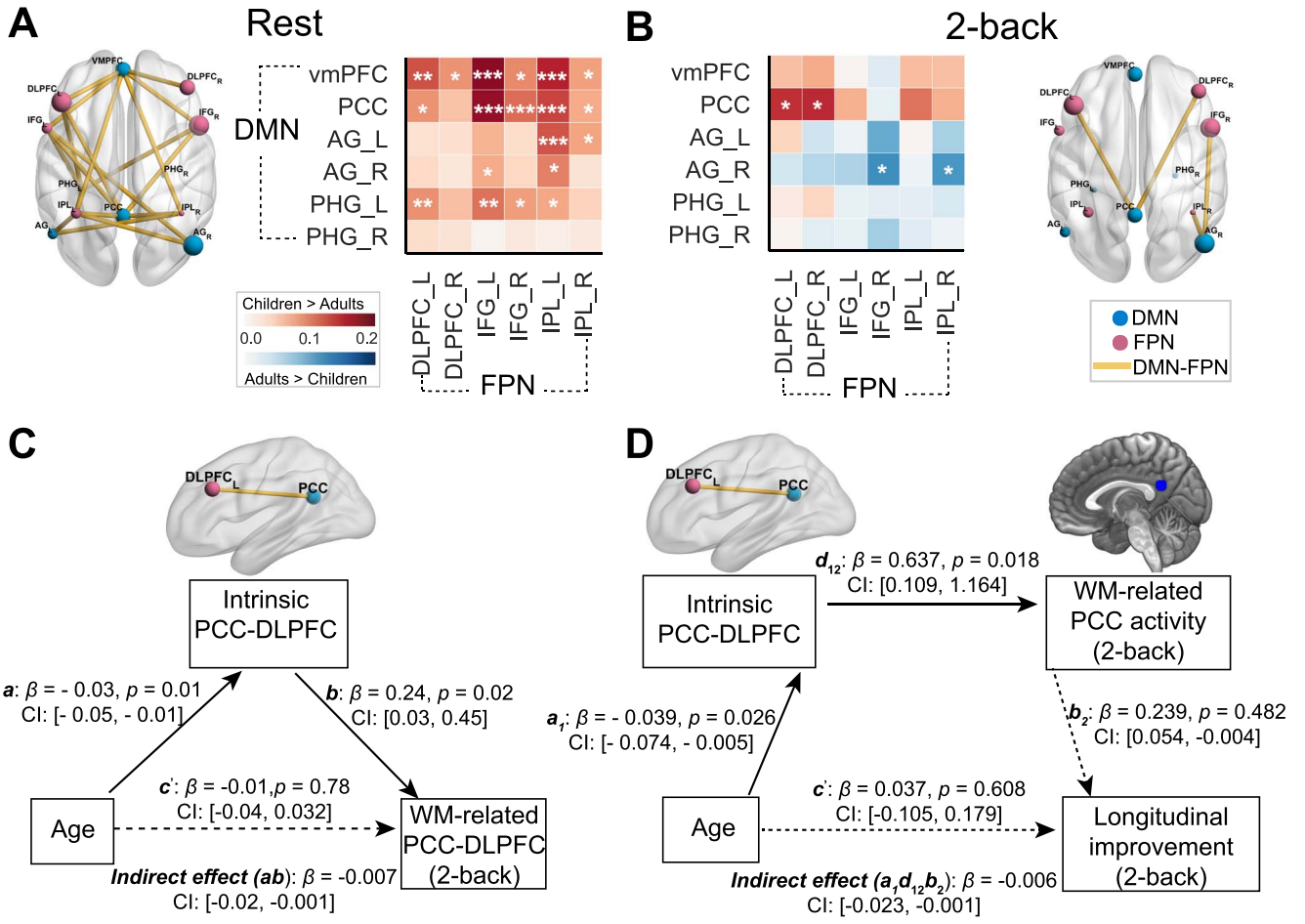

Fig. 5. Developmental differences in DMN-FPN coupling links and relationship with children's longitudinal working memory improvement. A) DMN-FPN intrinsic links that were significantly higher in children than adults ($q < 0.05$ FDR corrected). B) Working memory-related PCC-DLPFC coupling that was significantly higher in children than adults ($P < 0.05$ FDR corrected). C) A mediation model shows the mediatory effect of intrinsic PCC-DLPFC coupling that could account for an indirect association between children's age and working memory-related PCC-DLPFC coupling. D) A chain mediation model shows the mediatory effect of intrinsic PCC-DLPFC coupling and working memory-related PCC activity that could partially account for children's age-related longitudinal improvement in working memory RTs. Notes: DLPFC, dorsolateral prefrontal cortex; *, $P < 0.05$; **, $P < 0.01$; ***, $P < 0.001$.

a prominent longitudinal improvement from 6 to 15 years of age. Children exhibited less pronounced deactivation in DMN and weaker activation in FPN regions during working memory processing compared with adults. Children's DMN multivoxel activity and intranetwork connectivity reached an adult-like level earlier than FPN. Stronger DMN-FPN intrinsic coupling mediated task-dependent coordination of these networks during working memory in children, which further accounted for age-related improvements in working memory performance. Critically, PCC-DLPFC coupling emerged as a prominent pathway, and intrinsic PCC-DLPFC coupling further worked together with task-invoked PCC activity to account for longitudinal improvements in working memory performance. These findings highlight heterogeneous maturation patterns of the DMN and FPN involved in working memory and suggest that the DMN may provide a scaffold for an immature FPN to support working memory development.

Heterogeneous maturation of DMN and FPN involved in working memory

At a behavioral level, children exhibited inferior working memory performance as measured by accuracy and RTs, with prominent longitudinal improvement from 6 to 15 years. These findings are consistent with previous reports (Crone et al. 2006; Satterthwaite et al. 2013; Huang et al. 2016) documenting the immaturity of executive functioning from middle through late childhood into adolescence. In parallel, children exhibited less pronounced DMN deactivation and weaker FPN activation during working memory than adults. Active engagement of the FPN regions (i.e. DLPFC, inferior parietal lobule: IPL) is critical for information maintenance and updating during working memory processing, while engagement of the DMN regions (i.e. PCC, MPFC) could also contribute to attending internal task relevant information and disregarding current perceptual inputs during retrieving phase (Smallwood et al. 2013; Liu et al. 2016). These networks both playing important roles in working memory; task performance has been linked to top-down control of FPN over DMN to flexibly reallocate neurocognitive resources for working memory processing (Chen et al. 2013). Thus, our observations on DMN and FPN function may reflect immature neurofunctional organization involved in working memory processing in children.

Beyond univariate data, our multivariate maturation analysis revealed that children's DMN reached an adult-like level at ages 6–12, while the FPN still underwent a protracted development. Such heterogeneity is reminiscent of previous findings of anatomical properties (i.e. gray matter volumes, cortical thickness) in DMN structures that mature earlier than FPN (Sowell et al. 1999; Casey et al. 2000; Lenroot and Giedd 2006). Evidence from topographical organization also supports earlier maturation of the

DMN than FPN, as the FPN is anchored in higher order prefrontal and parietal association cortices (Klingberg et al. 2002). Based on the neurocognitive accounts of RSA, this measure indexes similarity of multivoxel activity patterns representing multiple cognitive components of working memory between children and adults (Freund et al. 2021). We thus speculate that our observed adult-like level of working memory-related multivoxel activity patterns in children may reflect that this system acts in a mature manner to support information processing during working memory. The observed earlier maturation of DMN structures as young as 7–9 years (Fair et al. 2008; Sherman et al. 2014) lends supports to this speculation.

Maturational changes in intra- and inter-network coupling of DMN and FPN

At a network level, children's DMN intranetwork coupling during both a working memory task and resting states reached an adult-like level, but this was not the case in the FPN. This is in line with resting-state fMRI findings suggesting that the DMN acts as a cohesive system with greater integration within its internal nodes in school-aged children (Gu et al. 2015). By extending previous findings (Cole et al. 2014), children's adult-like DMN intranetwork coupling could be attributed to an early beginning myelination and structural organization of axonal tracts among DMN structures (Fair et al. 2008; Supekar et al. 2010). Likewise, the DMN's small-world configuration with rich clubs emerges in childhood (Ball et al. 2014; Degnan et al. 2015), showing high internal synchronization to facilitate the convergence of internal and external information to support cognitive tasks (Raichle et al. 2001; Vatansever et al. 2015). With regards to children's weaker FPN intranetwork coupling, this suggests immature functional architecture of this network at ages 6–12. This concurs with a protracted development of structural and functional connections among FPN nodes (Fair et al. 2007).

Despite weaker FPN intranetwork coupling, children exhibited higher DMN internetwork coupling with FPN regions during both a working memory task and resting states. Over development, brain networks become gradually segregated and organized into finer-grained modules (Fair et al. 2009; Baum et al. 2017). Children's higher DMN coupling with FPN may reflect immature, less pronounced segregation among regions of these networks. Differences of networks' coupling between children and adults suggest that nuanced coordination of DMN with FPN may enable flexible information exchange and updating in working memory. A similar pattern of stronger DMN coupling with FPN has been linked to better memory performance in adults (van Buuren et al. 2019), and enhanced DMN coupling could compensate for age-associated memory impairment (Sambataro et al. 2010). We thus speculate a similar mechanism might be involved in aiding children's working memory processing, likely through stronger DMN coupling with an immature FPN. This speculation is further supported by our brain–behavior associations discussed below.

DMN scaffolds the relatively slower maturity of FPN to support working memory performance

In conjunction with overall DMN-FPN coupling, we further identified that PPC-DLPFC coupling emerged as a prominent pathway to mediate task-invoked coupling during working memory. Critically, we observed a chain mediating effect—that is, younger children exhibited stronger intrinsic coupling of this pathway together with higher task-invoked activity in the PCC to account for longitudinal improvement in working memory performance. These findings are in agreement with recent neurocognitive views suggesting activity flow over intrinsic functional pathways underlies task-related activity and behavioral performance (Cole et al. 2016; Tavor et al. 2016). By extending previous findings, we take one step further to speculate that the PCC-DLPFC pathway emerges as a particularly necessary route to confer the scaffolding role of the DMN in cooperating with an immature FPN during working memory processing (Baum et al. 2020).

As the central hubs of DMN and FPN, PCC and DLPFC are indispensable to support internally oriented processes (i.e. self-referenced and embodied cognition) (Raichle 2015) and executive functioning including working memory, respectively (Curtis and D'Esposito 2003). The PCC is posited as an active locus that continuously gathers and broadcasts information about one's internal state and the external inputs (Raichle et al. 2001). Indeed, the use of embodied procedures by linking to one's episodic experiences can effectively facilitate the development of more advanced and efficient problem-solving skills (Siegler 1996; Butterworth 1999; Qin et al. 2014). It is thus possible that the involvement of these processes, as reflected by PCC-DLPFC coupling and task-evoked PCC activity linked to longitudinal working memory improvements of RTs in the 2-back condition, could provide a scaffold for immature DLPFC-mediated executive functioning in younger children. Multiple lines of previous research have suggested that the DMN can act as a workspace for convergence of memory-based information and generating top-down predictions over external inputs (Deniz et al. 2017) to support global information integration including self-involved and embodied processes, episodic experiences, social, and other cognitive demands in the mature brain (Vatansever et al. 2015; Deniz et al. 2017; Sormaz et al. 2018). As such, it is conceivable to speculate that the PCC, as an important hub in DMN, could scaffold executive function under the workspace framework. Since previous findings have suggested a compensatory contribution of DMN to scaffolding aging-related decline in FPN regions critical for higher-order cognition including working memory (Spreng and Schacter 2012, Spreng and Turner 2019, Kupis et al. 2021), we thus speculate a similar mechanism that might be relevant to account for our observed developmental effects on DMN and FPN regions here. That is, an earlier maturation of the DMN may play a role in scaffolding the relatively slower yet immature FPN, likely through use of DMN-driven self-referential and embodied processes, along with its role in convergence of internal and external information (Kaefer et al., 2022) to support working memory processing in the developing brain.

There are several limitations to note in the current study. First, our study did not cover a complete developmental period from childhood through adolescence into adulthood. Second, we used a classical *n*-back paradigm to probe how the interplay of DMN with FPN contributes to children's working memory processing. Whether our findings can be generalized to other executive function domains remains open. Third, the DMN's role in scaffolding an immature FPN during working memory in childhood still remains speculative. Future studies with novel designs and advanced techniques are required to determine the causal links supporting this interpretation. Finally, as an essential task design feature of longitudinal study, repeated testing is also related with confounding data such as practice effects, which are worth considering in future studies.

In conclusion, our study demonstrates heterogeneous maturation of the DMN and FPN involved in working memory at both multivoxel activity and network organization levels. Children's DMN reaches an adult-like maturation earlier than FPN. We suggest that the DMN could provide a scaffold for the FPN's

relatively slower maturity to support children's working memory processing. Our findings provide important insights into the multifaceted contributions of the DMN to human cognition from a developmental perspective, which can inform future research to uncover the organizational principles of how the DMN works in concert with FPN to support cognitive development more broadly.

Acknowledgments

We thank the National Center for Protein Sciences at Peking University in Beijing, China, for assistance with MRI data acquisition.

Supplementary material

Supplementary material is available at *Cerebral Cortex* online.

Funding

National Natural Science Foundation of China (32200871, 32130045, 82021004, 31522028, 81571056); The Beijing Brain Initiative of Beijing Municipal Science & Technology Commission (Z181100001518003); Open Research Fund of the State Key Laboratory of Cognitive Neuroscience and Learning (CNLZD1503, CNLZD1703); Major Project of National Social Science Foundation (19ZDA363, 20&ZD153); 111 Project (BP0719032); National Key Research and Development Program of China (2022ZD0211000); National Institute on Drug Abuse (U01DA050987 to LQU).

Conflict of interest statement: None declared.

Authors' contributions

SQ, ST, YH, JG, ST, and QD designed research; MC, YH, LH, JX, TT, GZ, JL, YZ, and MJ performed research; MC, YH and LH analyzed data; MC, YH and SQ wrote the manuscript; all authors commented and edited the manuscript.

References

Alvarez JA, Emory E. Executive function and the frontal lobes: a meta-analytic review. *Neuropsychol Rev*. 2006:16(1):17–42. https://doi.org/10.1007/s11065-006-9002-x.

Ball G, Aljabar P, Zebari S, Tusor N, Arichi T, Merchant N, Robinson EC, Ogundipe E, Rueckert D, Edwards AD, et al. Rich-club organization of the newborn human brain. *Proc Natl Acad Sci*. 2014:111(20):7456–7461. https://doi.org/10.1073/pnas.1324118111.

Baum GL, Ciric R, Roalf DR, Betzel RF, Moore TM, Shinohara RT, Kahn AE, Vandekar SN, Rupert PE, Quarmley M, et al. Modular segregation of structural brain networks supports the development of executive function in youth. *Curr Biol*. 2017:27(11):1561–1572.e8. https://doi.org/10.1016/j.cub.2017.04.051.

Baum GL, Cui Z, Roalf DR, Ciric R, Betzel RF, Larsen B, Cieslak M, Cook PA, Xia CH, Moore TM, et al. Development of structure–function coupling in human brain networks during youth. *Proc Natl Acad Sci U S A*. 2020:117(1):771–778. https://doi.org/10.1073/pnas.1912034117.

Buckner RL, Krienen FM. The evolution of distributed association networks in the human brain. *Trends Cogn Sci*. 2013:17(12):648–665.

Buckner RL, Andrews-Hanna JR, Schacter DL. The brains default network: Anatomy, function, and relevance to disease. *Ann NY Acad Sci*. 2008:1124(1):138.

Butterworth B. *The mathematical brain*. London, Macmillan; 1999.

van Buuren M, Wagner IC, Fernández G. Functional network interactions at rest underlie individual differences in memory ability. *Learn Mem*. 2019:26(1):9–19. https://doi.org/10.1101/lm.048199.118.

Casey BJ, Giedd JN, Thomas KM. Structural and functional brain development and its relation to cognitive development. *Biol Psychol*. 2000:54(1–3):241–257. https://doi.org/10.1016/S0301-0511(00)00058-2.

Casey B, Tottenham N, Liston C, Durston S. Imaging the developing brain: what have we learned about cognitive development? *Trends Cogn Sci*. 2005:9(3):104–110. https://doi.org/10.1016/j.tics.2005.01.011.

Chen AC, Oathes DJ, Chang C, Bradley T, Zhou Z-W, Williams LM, Glover GH, Deisseroth K, Etkin A. Causal interactions between fronto-parietal central executive and default-mode networks in humans. *PNAS*. 2013:110(49):19944–19949. https://doi.org/10.1073/pnas.1311772110.

Cole MW, Bassett DS, Power JD, Braver TS, Petersen SE. Intrinsic and task-evoked network architectures of the human brain. *Neuron*. 2014:83(1):238–251. https://doi.org/10.1016/j.neuron.2014.05.014.

Cole MW, Ito T, Bassett DS, Schultz DH. Activity flow over resting-state networks shapes cognitive task activations. *Nat Neurosci*. 2016:19(12):1718–1726. https://doi.org/10.1038/nn.4406.

Crone EA, Wendelken C, Donohue S, van Leijenhorst L, Bunge SA. Neurocognitive development of the ability to manipulate information in working memory. *Proc Natl Acad Sci*. 2006:103(24):9315–9320. https://doi.org/10.1073/pnas.0510088103.

Curtis CE, D'Esposito M. Persistent activity in the prefrontal cortex during working memory. *Trends Cogn Sci*. 2003:7(9):415–423. https://doi.org/10.1016/S1364-6613(03)00197-9.

Degnan AJ, Wisnowski JL, Choi S, Ceschin R, Bhushan C, Leahy RM, Corby P, Schmithorst VJ, Panigrahy A. Altered structural and functional connectivity in late preterm preadolescence: an anatomic seed-based study of resting state networks related to the posteromedial and lateral parietal cortex. *PLoS One*. 2015:10(6):e0130686. https://doi.org/10.1371/journal.pone.0130686.

Deniz V, Menon DK, Stamatakis EA. Default mode contributions to automated information processing. *Proc Natl Acad Sci U S A*. 2017:114(48):12821–12826. https://doi.org/10.1073/pnas.1710521114.

Di Martino A, Fair DA, Kelly C, Satterthwaite TD, Castellanos FX, Thomason ME, Craddock RC, Luna B, Leventhal BL, Zuo X-N, et al. Unraveling the Miswired connectome: a developmental perspective. *Neuron*. 2014:83(6):1335–1353. https://doi.org/10.1016/j.neuron.2014.08.050.

Dosenbach NUF, Fair DA, Cohen AL, Schlaggar BL, Petersen SE. A dual-networks architecture of top-down control. *Trends Cogn Sci*. 2008:12(3):99–105.

Fair DA, Dosenbach NUF, Church JA, Cohen AL, Brahmbhatt S, Miezin FM, Barch DM, Raichle ME, Petersen SE, Schlaggar BL. Development of distinct control networks through segregation and integration. *PNAS*. 2007:104(33):13507–13512. https://doi.org/10.1073/pnas.0705843104.

Fair DA, Cohen AL, Dosenbach NUF, Church JA, Miezin FM, Barch DM, Raichle ME, Petersen SE, Schlaggar BL. The maturing architecture of the brain's default network. *Proc Natl Acad Sci*. 2008:105(10):4028–4032. https://doi.org/10.1073/pnas.0800376105.

Fair DA, Cohen AL, Power JD, Dosenbach NUF, Church JA, Miezin FM, Schlaggar BL, Petersen SE. Functional brain networks develop from a "local to distributed" organization. *PLoS*

Comput Biol. 2009:5(5):e1000381. https://doi.org/10.1371/journal.pcbi.1000381.

Fornito A, Harrison BJ, Zalesky A, Simons JS. Competitive and cooperative dynamics of large-scale brain functional networks supporting recollection. *Proc Natl Acad Sci*. 2012:109(31):12788–12793. https://doi.org/10.1073/pnas.1204185109.

Freund MC, Etzel JA, Braver TS. Neural coding of cognitive control: the representational similarity analysis approach. *Trends Cogn Sci*. 2021:25(7):622–638.

Friston KJ, Holmes AP, Worsley KJ, Poline J-P, Frith CD, Frackowiak RSJ. Statistical parametric maps in functional imaging: a general linear approach. *Hum Brain Mapp*. 1994:2(4):189–210. https://doi.org/10.1002/hbm.460020402.

Grayson DS, Fair DA. Development of large-scale functional networks from birth to adulthood: a guide to the neuroimaging literature. *NeuroImage*. 2017:160:15–31. https://doi.org/10.1016/j.neuroimage.2017.01.079.

Gu S, Satterthwaite TD, Medaglia JD, Yang M, Gur RE, Gur RC, Bassett DS. Emergence of system roles in normative neurodevelopment. *Proc Natl Acad Sci U S A*. 2015:112(44):13681–13686. https://doi.org/10.1073/pnas.1502829112.

Haggard P. Human volition: towards a neuroscience of will. *Nat Rev Neurosci*. 2008:9(12):934–946. https://doi.org/10.1038/nrn2497.

Hartwigsen G. Flexible redistribution in cognitive networks. *Trends Cogn Sci*. 2018:22(8):687–698. https://doi.org/10.1016/j.tics.2018.05.008.

Hayes AF. *Introduction to mediation, moderation, and conditional process analysis: a regression-based approach*. New York: The Guilford Press (Methodology in the social sciences); 2013.

Huang AS, Klein DN, Leung H-C. Load-related brain activation predicts spatial working memory performance in youth aged 9–12 and is associated with executive function at earlier ages. *Dev Cogn Neurosci*. 2016:100(17):1–9. https://doi.org/10.1016/j.dcn.2015.10.007.

Ivanova A, Zaidel E, Salamon N, Bookheimer S, Uddin LQ, de Bode S. Intrinsic functional organization of putative language networks in the brain following left cerebral hemispherectomy. *Brain Struct Funct*. 2017:222(8):3795–3805. https://doi.org/10.1007/s00429-017-1434-y.

Johnson MH. Functional brain development in humans. *Nat Rev Neurosci*. 2001:2(7):475–483. https://doi.org/10.1038/35081509.

Johnson MH. Interactive specialization: a domain-general framework for human functional brain development? *Dev Cogn Neurosci*. 2011:1(1):7–21. https://doi.org/10.1016/j.dcn.2010.07.003.

Kaefer K, Stella F, McNaughton BL, et al. Replay, the default mode network and the cascaded memory systems model. Nat Rev Neurosci. 2002:23:628–640. https://doi.org/10.1038/s41583-022-00620-6

Klingberg T, Forssberg H, Westerberg H. Increased brain activity in frontal and parietal cortex underlies the development of visuospatial working memory capacity during childhood. *J Cogn Neurosci*. 2002:14(1):1–10. https://doi.org/10.1162/089892902317205276.

Krieger-Redwood K, Jefferies E, Karapanagiotidis T, Seymour R, Nunes A, Ang JWA, Majernikova V, Mollo G, Smallwood J. Down but not out in posterior cingulate cortex: deactivation yet functional coupling with prefrontal cortex during demanding semantic cognition. *NeuroImage*. 2016:100(141):366–377. https://doi.org/10.1016/j.neuroimage.2016.07.060.

Kriegeskorte N, Mur M, Bandettini PA. Representational similarity analysis-connecting the branches of systems neuroscience. *Front Syst Neurosci*. 2008:2:4.

Kupis L, Goodman ZT, Kornfeld S, Hoang S, Romero C, Dirks B, Dehoney J, Chang C, Spreng RN, Nomi JS, et al. Brain dynamics underlying cognitive flexibility across the lifespan. *Cereb Cortex*. 2021:31(11):5263–5274. https://doi.org/10.1093/cercor/bhab156.

Lenroot RK, Giedd JN. Brain development in children and adolescents: insights from anatomical magnetic resonance imaging. *Neurosci Biobehav Rev*. 2006:30(6):718–729. https://doi.org/10.1016/j.neubiorev.2006.06.001.

Liu Y, Lin W, Liu C. et al. Memory consolidation reconfigures neural pathways involved in the suppression of emotional memories. *Nat Commun* 7, 13375 (2016). https://doi.org/10.1038/ncomms13375

Lustig C, Snyder A, Bhakta M, O'Brien KC, McAvoy M, Raichle M, Morris J, Buckner R. Functional deactivations: change with age and dementia of the Alzheimer type. *Proc Natl Acad Sci U S A*. 2003:100(24):14504–14509.

Marek S, Hwang K, Foran W, Hallquist MN, Luna B. The contribution of network organization and integration to the development of cognitive control. *PLoS Biol*. 2015:13(12):e1002328.

Margulies DS, Ghosh SS, Goulas A, Falkiewicz M, Huntenburg JM, Langs G, Bezgin G, Eickhoff SB, Castellanos FX, Petrides M, et al. Situating the default-mode network along a principal gradient of macroscale cortical organization. *Proc Natl Acad Sci U S A*. 2016:113(44):12574–12579. https://doi.org/10.1073/pnas.1608282113.

McLaren DG, Ries ML, Xu G, Johnson SC. A generalized form of context-dependent psychophysiological interactions (gPPI): a comparison to standard approaches. *NeuroImage*. 2012:61(4):1277–1286. https://doi.org/10.1016/j.neuroimage.2012.03.068.

Mürner-Lavanchy I, Ritter BC, Spencer-Smith MM, Perrig WJ, Schroth G, Steinlin M, Everts R. Visuospatial working memory in very preterm and term born children—impact of age and performance. *Dev Cogn Neurosci*. 2014:9:106–116. https://doi.org/10.1016/j.dcn.2014.02.004.

Nelson SM, Savalia NK, Fishell AK, Gilmore AW, Zou F, Balota DA, McDermott KB. Default mode network activity predicts early memory decline in healthy young adults aged 18-31. *Cereb Cortex*. 2016:26(8):3379–3389. https://doi.org/10.1093/cercor/bhv165.

Olesen PJ, Nagy Z, Westerberg H, Klingberg T. Combined analysis of DTI and fMRI data reveals a joint maturation of white and grey matter in a fronto-parietal network. *Cogn Brain Res*. 2003:18(1):48–57. https://doi.org/10.1016/j.cogbrainres.2003.09.003.

Park DC, Reuter-Lorenz P. The adaptive brain: aging and neurocognitive scaffolding. *Annu Rev Psychol*. 2009:60(1):173–196. https://doi.org/10.1146/annurev.psych.59.103006.093656.

Pinheiro J, Bates D, DebRoy S, Sarkar D, Team RC. *Nlme: linear and nonlinear mixed effects models. R package version 3.1–137*. Vienna, Austria: R Foundation; 2018.

Posner M, Petersen S, Fox P, Raichle M. Localization of cognitive operations in the human brain. *Science*. 1988:240(4859):1627–1631. https://doi.org/10.1126/science.3289116.

Power JD, Fair DA, Schlaggar BL, Petersen SE. The development of human functional brain networks. *Neuron*. 2010:67(5):735–748. https://doi.org/10.1016/j.neuron.2010.08.017.

Preacher KJ, Hayes AF. Asymptotic and resampling strategies for assessing and comparing indirect effects in multiple mediator models. *Behav Res Methods*. 2008:40(3):879–891. https://doi.org/10.3758/BRM.40.3.879.

Qin S, Cho S, Chen T, Rosenberg-Lee M, Geary DC, Menon V. Hippocampal-neocortical functional reorganization underlies children's cognitive development. *Nat Neurosci*. 2014:17(9):1263–1269.

Raichle ME. The Brain's default mode network. *Annu Rev Neurosci*. 2015:38(1):433–447. https://doi.org/10.1146/annurev-neuro-071013-014030.

Raichle ME, MacLeod AM, Snyder AZ, Powers WJ, Gusnard DA, Shulman GL. A default mode of brain function. *Proc Natl Acad Sci*. 2001:98(2):676–682. https://doi.org/10.1073/pnas.98.2.676.

Sambataro F, Murty VP, Callicott JH, Tan HY, Das S, Weinberger DR, Mattay VS. Age-related alterations in default mode network: impact on working memory performance. *Neurobiol Aging*. 2010:31(5):839–852. https://doi.org/10.1016/j.neurobiolaging.2008.05.022.

Satterthwaite TD, Wolf DH, Erus G, Ruparel K, Elliott MA, Gennatas ED, Hopson R, Jackson C, Prabhakaran K, Bilker WB, et al. Functional maturation of the executive system during adolescence. *J Neurosci*. 2013:33(41):16249–16261. https://doi.org/10.1523/JNEUROSCI.2345-13.2013.

Sherman LE, Rudie JD, Pfeifer JH, Masten CL, McNealy K, Dapretto M. Development of the default mode and central executive networks across early adolescence: a longitudinal study. *Dev Cogn Neurosci*. 2014:10:148–159. https://doi.org/10.1016/j.dcn.2014.08.002.

Shine JM, Bissett PG, Bell PT, Koyejo O, Balsters JH, Gorgolewski KJ, Moodie CA, Poldrack RA. The dynamics of functional brain networks: integrated network states during cognitive task performance. *Neuron*. 2016:92(2):544–554. https://doi.org/10.1016/j.neuron.2016.09.018.

Siegler RS. *Emerging minds: the process of change in children's thinking*. New York, NY, US: Oxford University Press; 1996

Smallwood J, Tipper C, Brown K, Baird B, Engen H, Michaels JR, Grafton S, Schooler JW. Escaping the here and now: evidence for a role of the default mode network in perceptually decoupled thought. *NeuroImage*. 2013:69:120–125. https://doi.org/10.1016/j.neuroimage.2012.12.012.

Smallwood J, Bernhardt BC, Leech R, Bzdok D, Jefferies E, Margulies DS. The default mode network in cognition: a topographical perspective. *Nat Rev Neurosci*. 2021:22(8):503–513. https://doi.org/10.1038/s41583-021-00474-4.

Sormaz M, Murphy C, Wang H, Hymers M, Karapanagiotidis T, Poerio G, Margulies DS, Jefferies E, Smallwood J. Default mode network can support the level of detail in experience during active task states. *Proc Natl Acad Sci U S A*. 2018:115(37):9318–9323. https://doi.org/10.1073/pnas.1721259115.

Sowell ER, Thompson PM, Holmes CJ, Jernigan TL, Toga AW. In vivo evidence for post-adolescent brain maturation in frontal and striatal regions. *Nat Neurosci*. 1999:2(10):859–861. https://doi.org/10.1038/13154.

Spreng RN, Schacter DL. Default network modulation and large-scale network interactivity in healthy young and old adults. *Cereb Cortex*. 2012:22(11):2610–2621. https://doi.org/10.1093/cercor/bhr339.

Spreng RN, Turner GR. The shifting architecture of cognition and brain function in older adulthood. *Perspect Psychol Sci*. 2019:14(4):523–542. https://doi.org/10.1177/1745691619827511.

Supekar K, Musen M, Menon V. Development of large-scale functional brain networks in children. *PLoS Biol*. 2009:7(7):15.

Supekar K, Uddin LQ, Prater K, Amin H, Greicius MD, Menon V. Development of functional and structural connectivity within the default mode network in young children. *NeuroImage*. 2010:52(1):290–301. https://doi.org/10.1016/j.neuroimage.2010.04.009.

Tavor I, Jones OP, Mars RB, Smith SM, Behrens TE, Jbabdi S. Task-free MRI predicts individual differences in brain activity during task performance. *Science*. 2016:352(6282):216–220. https://doi.org/10.1126/science.aad8127.

Team RC. *R: a language and environment for statistical computing*. R Foundation for Statistical Computing. Vienna, Austria. 2018.

Uddin LQ, Supekar KS, Ryali S, Menon V. Dynamic reconfiguration of structural and functional connectivity across Core neurocognitive brain networks with development. *J Neurosci*. 2011:31(50):18578–18589. https://doi.org/10.1523/JNEUROSCI.4465-11.2011.

Uddin LQ, Yeo BTT, Spreng RN. Towards a universal taxonomy of macro-scale functional human brain networks. *Brain Topogr*. 2019:32(6):926–942. https://doi.org/10.1007/s10548-019-00744-6.

Vatansever D, Menon DK, Manktelow AE, Sahakian BJ, Stamatakis EA. Default mode dynamics for global functional integration. *J Neurosci*. 2015:35(46):15254–15262. https://doi.org/10.1523/JNEUROSCI.2135-15.2015.

Vatansever D, Manktelow AE, Sahakian BJ, Menon DK, Stamatakis EA. Angular default mode network connectivity across working memory load. *Hum Brain Mapp*. 2017:38(1):41–52. https://doi.org/10.1002/hbm.23341.

Yeshurun Y, Nguyen M, Hasson U. The default mode network: where the idiosyncratic self meets the shared social world. *Nat Rev Neurosci*. 2021:22(March):181–192. https://doi.org/10.1038/s41583-020-00420-w.

Zhuang L, Wang J, Xiong B, Bian C, Hao L, Bayley PJ, Qin S. Rapid neural reorganization during retrieval practice predicts subsequent long-term retention and false memory. *Nat Hum Behav*. 2022:6(1):134–145. https://doi.org/10.1038/s41562-021-01188-4.